SIMULATION OF PROJECTILE IMPACT ON LAYERED PACKAGE MADE OF UNIDIRECTIONAL GLASS FIBERS

Larisa CHIPER TITIRE[1], George Ghiocel OJOC[2],
Cătălin PÎRVU[3], Lorena DELEANU[4]

Particularities of impact simulation result from applying the load only once. The designed protection system is requested not to fail once or for a small number of hits. Tests for evaluating impact protection are expensive and numerous. In the literature, there are models at the meso level (multi-fiber yarns, layers of yarns, as is the case with this simulation). These help the engineers to restrain number and complexity of impact tests. This paper discusses the failure mechanisms and the stages for the simulated impact between a bullet (similar with 9 mm FMJ) and a package made of 4 layers of unidirectional yarns, having an architecture (0°,90°,0°,90°), for a range of impact velocity of 100...400 m/s. Simulations help to evaluate the residual velocity and, thus, to produce the first prototypes with a very high probability to resist. The analyses of the failure moments reveal the yarns' damage, depending on their positions with reference to the layer number (1 being for the first layer contacted by the projectile) and the projectile.

The simulation of impact on four-layer package pointed out the influence of impact velocity on maximum value of von Mises stress during the impact, on the acceleration-deceleration of the bullet tip. The simulation allows for evaluating the residual velocity and to compare its values to those obtained in actual tests. Also, the aspect of broken yarns, even if simulated for a compact yarn (not composed of numerous fibers), is similar to those obtained on SEM images for similar packages.

Keywords: impact, simulation, unidirectional glass fibers.

1. Introduction

The research for developing ballistic protection systems is consistent because today the war has becoming less a direct confrontation between two armies, but more a battle between disproportional forces and tactics, developed in economic, sanitary, military and social environments, for getting rapid and visible results [1], [2].

[1] Drd. eng., Dept. of Mechanical Engineering, "Dunarea de Jos" University of Galati, Romania, e-mail: chiper.larisa@yahoo.ro
[2] Drd. eng., Dept. of Mechanical Engineering, "Dunarea de Jos" University of Galati, Romania, e-mail: george.ojoc@ugal.ro
[3] Dr. eng., Flow Physics Department, National Institute of Aerospace Research "Elie Carafoli" (INCAS), Bucharest, Romania, e-mail: pirvu.catalin@incas.ro
[4] Prof., Dept. of Mechanical Engineering, "Dunarea de Jos" University of Galati, Romania, e-mail: lorena.deleanu@ugal.ro

The tensile strength of drawn glass fibers may exceed 3.45 GPa. However, surface defects caused by abrasion, either by friction between them or by contact with the production equipment, tend to reduce it to 1.72–2.07 GPa. Degradation of strength is accentuated as surface defects increase under cyclic loads, which is a major disadvantage of fiberglass in fatigue applications. The tensile strength of glass fibers is reduced in the presence of water. Water deepens surface defects, already present in fibers. Under continuous loading, the growth of surface defects is accelerated by corrosion, even by atmospheric humidity. As a result, the tensile strength of glass fibers decreases with increasing duration of use [3].

The unidirectional orientation of yarns in a composite produces the highest strength and modulus along fiber direction. Simple unidirectional fabrics are not used in protection systems because they do not offer resistance to penetration, the projectile easily removes secondary yarns (considered next to the yarns supporting direct contact with the projectile), but bi-axial and, more recently, quadriaxial layer fabrics, oriented (0°,90°,45°,-45°), are used. With an adequate orientation of fibers in successive layers, the difference in strength values in different directions can be reduced. Many laminates are prone to early breakage by delamination, in which cracks appeared at the interface between layers due to high interlaminar shear stresses [4], [5].

Glass fiber has been used in ballistic protection systems since the First World War. The development was taken over by the US Navy and the resulting product was a fiberglass shield, used in protective vests and for fixed or mobile equipment. Increasing the degree of protection of staff and equipment increases the chances of success for an intervention, but also its psychological support.

The aim of this paper is to simulate the behavior of unidirectional fabrics in order to use the model in the design of impact-resistant structures.

2. The Model of the System Target - Bullet, at Meso Level

The shape of the yarn cross section was selected after consulting [6]-[9] and it is similar to the shape of a quadriaxial glass fabrics (1200 g/m^2) [10], as shown in Fig. 1.

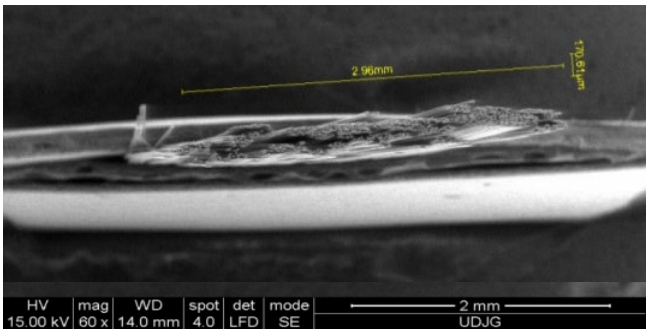

Fig. 1. Shape and dimensions of a glass yarn from a multi-axial fabrics.

Models for impact at meso level [11]-[14] raise meshing problems due to the very different dimensions of the bodies participating in the impact. In this model, the yarn has much larger dimensions on one axis (length) and similar dimensions, much smaller, on the other two axes. Figs. 2b and 3b present the mesh for yarns. Each yarn is considered clamped on its ends, on the side surface and its length is 60 mm, as shown in Fig. 2a.

Each yarn has the end surfaces rigidly clamped, as one may see in Fig. 2a, in darker blue color. The bullet is much larger than the cross thickness of the yarn and its meshing was done according to Fig. 2c. The yarn model is "linear EOS shock".

The bullet is considered to be made of two materials, the lead core and the jacket made of a copper alloy. Their properties are given in Table 1, values being selected after consulting [15]-[19].

The geometric model of the package (60 mm x 60 mm) is organized in four layers, each layer being composed of 20 unidirectional yarns, arranged (0°,90°,0°,90°). The yarn is modeled as in Fig. 2a, with a width of 3 mm and a thickness of 0.2 mm. The ends are rounded, with a radius equal to the half-height of the yarn. The model contains two planes of symmetry (Fig. 3a). Reducing the model to a quarter (Fig. 3a) will considerably reduce the computing time [12], [13]. The model contains 560421 nodes and 410407 elements (the size of the element being between 0.1 mm and 0.3 mm), and the constitutive model of the yarn material is isotropic bilinear, with characteristic values of the glass yarn. Table 1 presents the nodes and elements for each body.

Table 1

The bullet - unidirectional glass fiber fabric impact model

Body	Nodes	Elements
Jacket	1512	5524
Core	2140	9897
Bullet (Jacket + core)	3652	15421
1 layer	29498	20100
4 layers	556769	394986

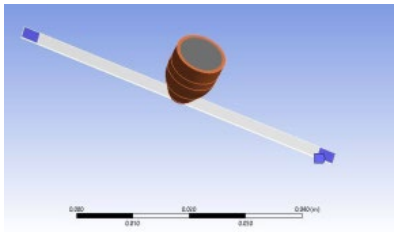

a) Modeling the conditions for lateral ends of the yarn

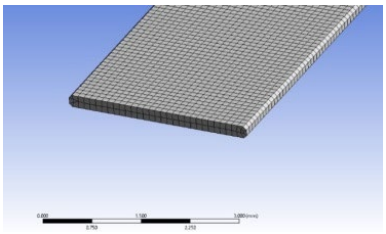

b) Yarn mesh

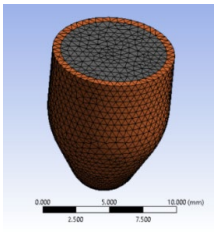

c) the projectile mesh

Fig. 2. Detail of the model

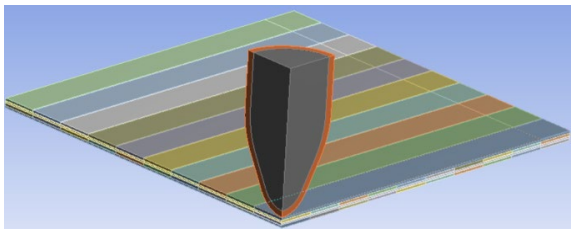

a) The model of system (a quarter of the package), built of 20 unidirectional yarns in a layer

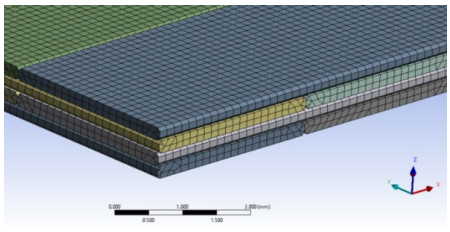

b) Detail of the meshing of the 4-layer package

Fig. 3. View of the modeled system

For this model, the following contact conditions are considered:

- the contact between the copper alloy jacket and the lead core of the projectile is "perfectly bonded",
- the contact between yarn and projectile is with friction; the friction coefficient between yarn and projectile was considered constant and equal to 0.3,
- the contact between yarns is with friction; the friction coefficient was considered constant and equal to 0.3.

Boundary conditions are related to the surfaces of each yarn ends (with 5 mm in the yarn length direction) that are rigidly clamped and the initial conditions refer to impact velocity (denoted by v_0) for four values: 100 m/s, 200 m/s, 300 m/s and 400 m/s.

Naresh et al. [15] presented experimental data on the influence of the strain rate of a glass fiber composite on the tensile strength limit for strain rates from 0.0016 s^{-1} to 542 s^{-1}. They found that the tensile limit and modulus of elasticity increased and the strain at break decreased for fiberglass composites.

This model considers a constitutive model of isotropic bilinear material for the glass yarn and, based on the resulting observations and experimental data from the literature [16]-[19], more complex constitutive models will be introduced to take into account the influence of the strain rate on strength, at high impact velocities. For example, Ou and Zhou [16] reported that the limit at break of a glass fiber composite increases substantially with increasing strain rate. Naik et al. [17] reported an increase in ultimate strength of 75–93% as compared to results obtained in the quasi-static test for fiberglass composites.

In a micro scale model of a polymer matrix composite, Patnaik et al. [18] used the following properties for fiberglass and then introduced the data obtained on this micro-composite model into a macro-model with several layers of composite: density 2400 kg/m^3, Young modulus 73 GPa, Poisson ratio 0.20, tensile strength 2300 MPa, fiber diameter 12 μm. However, the fraction of the fiber volume was relatively small, up to 27%, but in ballistic protection, composite systems could have this ratio towards 60…70%.

The objectives of this simulation study are the identification of failure stages of the package and the influence of the impact velocity on von Mises stress distribution, for the range of impact velocity of 100 m/s...400 m/s.

Based on the consulted literature, the following values were chosen for the properties of the glass yarn (here considered monoblock) (Table 2). Table 3 presents the analyzed cases and the moments of yarn(s) breaking.

Table 2

Mechanical properties of the yarn

Property	Yarn	Projectile	
		Core (lead)	Jacket (copper alloy)
Density, kg/m3	2540	11340	8300
Young modulus, MPa	1.13×10^5	0.2×10^5	1.17×10^5
Poisson ratio	0.25	0.43	0.34
Tangent modulus, MPa	12750	0	1150
Shear modulus, MPa	45200	6993	43657
Yield limit, MPa	919	30	70
Equivalent plastis strain at break (EPS)	0.03		

It is found that, when the impact velocity increases, the yarn break under the bullet is initiated at moments closer to the impact moment when the projectile contacts the target, the breaking of the yarn near the end of the yarn(s) starts later, at the moment $t=7.2\times10^{-5}$ s to $t=1.12\times10^{-5}$ s (for v_0=100 m/s to v_0=400 m/s). This failure by break of several yarns near their ends (that are rigidly clamped) is due to the model dimensions, resulting in a small area of the package, without matrix among yarns. Actual size of tested packages starts from 200 mm x 200 mm and standards require even 500 mm x 500 mm (EN 1522:1998 Windows, doors, shutters and blinds. Bullet resistance. Requirements and classification, EN 1523:1998 Windows, doors, shutters and blinds - Bullet resistance - Test method).

Table 3

Important moments for the simulated cases

Case	Impact velocity [m/s]	The moment of yarn break [s]	Number of broken yarns	Location
1	100	2.4×10^{-5}	2 yarns (layer 2 and 3)	Under the bullet
		7.2×10^{-5}	1 yarn (layer 4)	Failure(s) near the clamping area
2	200	8×10^{-6}	1 yarn (layer 1)	Under the bullet
		9.6×10^{-5}	1 yarn (layer 4)	Failure(s) near the clamping area
3	300	8×10^{-6}	3 yarns (layer 1, 2 and 3)	Under the bullet
		1.12×10^{-4}	1 yarn (layer 4)	Failure(s) near the clamping area
4	400	8×10^{-6}	3 yarns (layer 1, 2 and 3)	Under the bullet
		1.12×10^{-4}	1 yarn (layer 4)	Failure(s) near the clamping area

For this study, the equivalent plastic strain (EPS) is selected as the failure criterion. The criterion stipulates that failure (break) at a point in the material occurs when the equivalent plastic strain reaches a certain value, $\varepsilon^p = \varepsilon^p_{critical}$, in which $\varepsilon^p_{critical}$ is the plastic strain at break and it is a parameter that must be calibrated from the experimental data. The most common calibration test is the uniaxial tensile test, but shear tests can also be used [20].

Figure 4 presents the constitutive models for the involved materials.

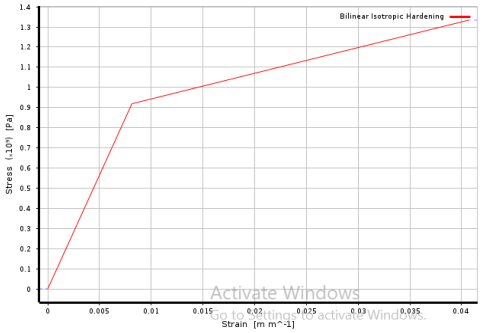

a) Isotropic bilinear model with hardening for fiberglass

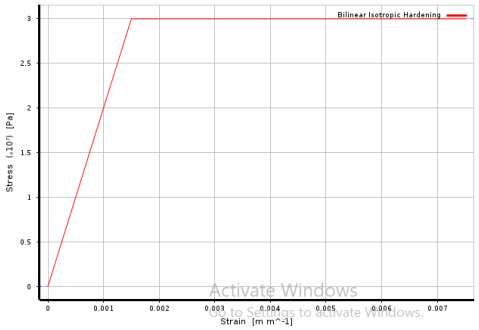

b) Isotropic bilinear model for lead (projectile core)

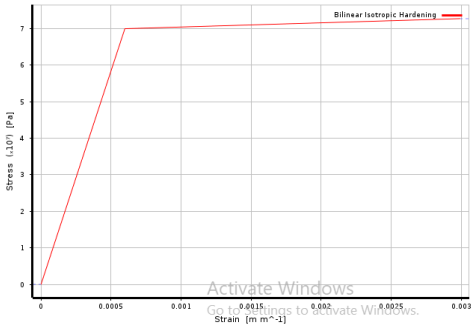

c) Isotropic bilinear model (with hardening) for copper alloy of the jacket

Fig. 4. The constitutive models for the materials involved in this simulation

3. Results and Discussion for Simulated Cases

Information obtained from running the model for four impact velocities included:

- graph of maximum von Mises stress in time, because stress values can give indications of yarns' damage,

- the velocity graph in time, because, from this information, it can result: the absorbed energy, the remaining energy of the bullet; if many runs are done it is possible to determine under what conditions the residual velocity becomes zero (the projectile is stopped),

- the acceleration of the bullet tip in time gives information on the impact force (considering that the projectile is not fragmented).

The maximum values of these graphs, correlated, may give information about the failure mechanisms of the yarn and the moments when they take place. The first break of the yarn(s) allows for the stress to decrease, but the yarn on the following layer opposes the projectile and it makes the stress to become higher.

For the four-layer package, the variation of the equivalent stress is in the range 1100-1300 MPa, over a longer period of time, $\Delta t=1.6\times10^{-4}$ s (taking into account the running time) (Fig. 5). First peak of the stress-time curves, reaching the strength limit, reflects the failure of the first yarn, usually from the first layer

In general, an acceleration peak will represent a failure mechanism, through which one or more yarns no longer oppose the penetration of the projectile (Fig. 6). These can be large plastic deformations (less often), breakings, twists of the secondary yarns etc.

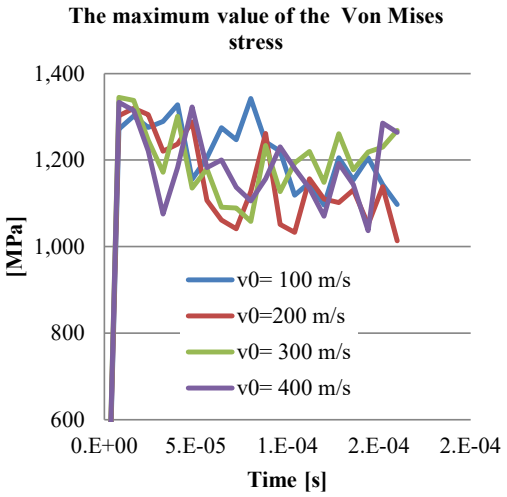

Fig. 5. Evolution in time of the maximum value for von Mises stress

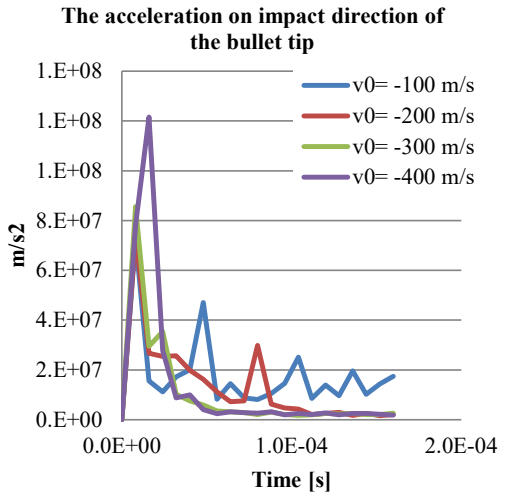

Fig. 6. Evolution of the bullet tip acceleration in the direction of impact

From Table 4, it is observed that, for low velocity, the velocity variation in percent is higher and at higher impact velocity, the variation in percent is smaller. Each velocity graph in time shows a major slowdown, but also an increase (this is corresponding to the major first peak of acceleration).

Table 4

Residual velocity for impact on the pan with 4 layers of unidirectional yarns.

Case	v_0 [m/s]	Residual velocity at the end of the simulation [m/s]	Variation in percent [%]
4 yarns (0°,90°,0°,90°)	100	92.76	7.24
	200	195.89	2.055
	300	294.54	1.82
	400	394.33	1.42

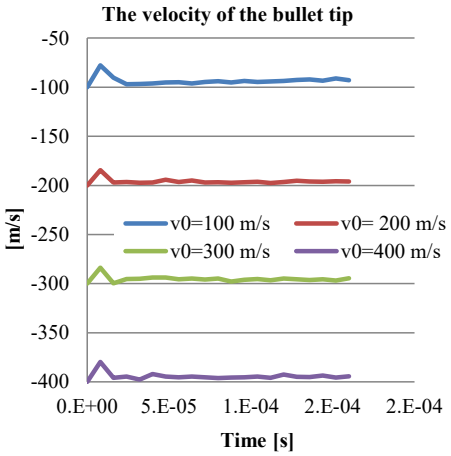

Fig. 7. Evolution of proiectile tip velocity, for different impact velocities

This simulation could be run for more layers in order to obtained a residual velocity close to zero. For this thickness of the packages could start the laboratory test and, depending on the target response, the package will vary its thickness, but in a narrow range due to preliminary results from simulation.

4. Analysis of Yarn Failure Mechanisms for Each Case

In the analysis of fabrics damages, the yarns that break under the bullet (Fig. 8) are called main yarns and the yarns that are only removed, deformed, twisted due to the passage of the bullet through the package are called secondary yarns.

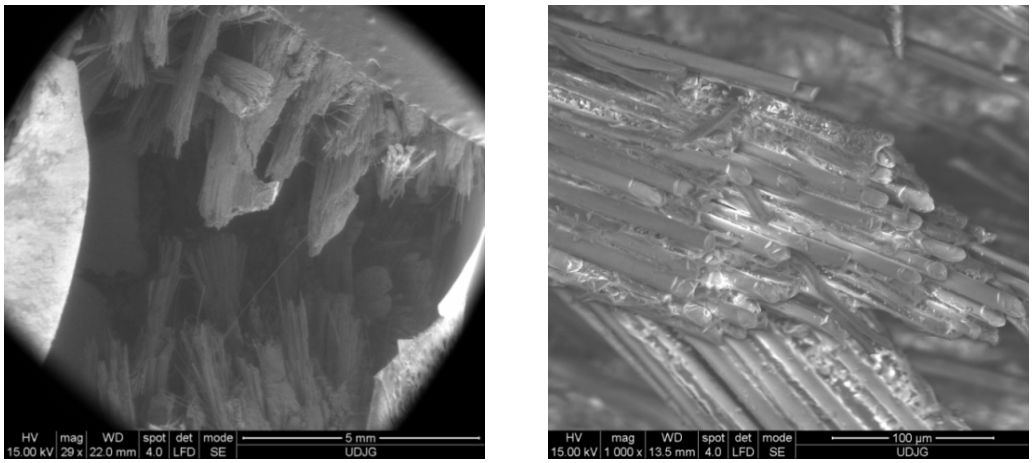

a) near the bullet b) detail of the broken yarn in the same zone

Fig. 8. Aspect of failure of fiberglass yarns after the impact with v_0 = 400 m/s (level FB3) [21]

The failure mechanisms identified on the simulation, for this package with 4 layers of unidirectional glass yarns are:

- yarn compression and shear, under the bullet,
- the failure due to tensile stress, at the edge of the contact,
- the yarns' failure through bending, arching them (near the impacted area, when the bullet passes by the broken yarns).

For a more detailed study, Ansys offers the possibility to make transparent one or more bodies in the modeled system.

The figures 9, 11, 13 and 15 show the distribution of equivalent stresses on the analyzed package, for each impact velocity. Images in Figures 10, 12, 14 and 16 were obtained keeping visible only one layer of interest and making the other layers invisible and they reveal differences in how each layer is stressed and damaged.

At v_0=100 m/s and the moment t=2.4×10^{-5} s (Fig. 9), layer 1 has a yarn almost broken, in several fragments, layer 2 and layer 3 have a broken yarn, the rupture being almost parallel to the yarn width. Layer 4 has no broken yarns, yet.

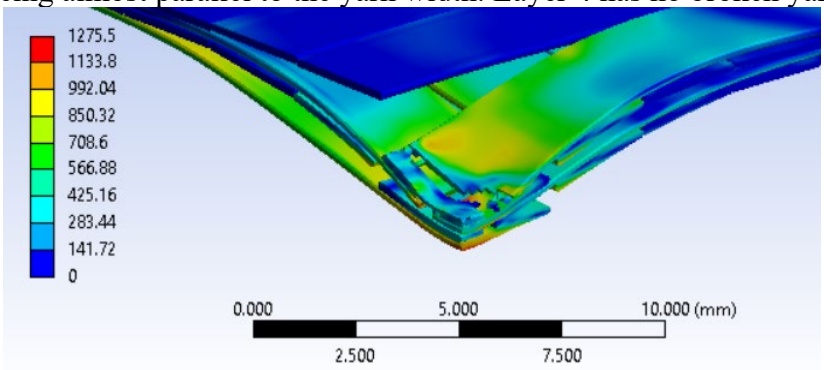

Fig. 9. Von Mises stress distribution (in MPa) and failure aspect at moment, t=2.4×10^{-5} s, for v_0=100 m/s

Making visible only a layer (Fig. 10), one may notice: a) a central detached piece from the yarn on layer 1, in contact with the projectile and small fragments, b) and c) yarns on layer 2 and layer 3 are broken and bended, the contact between yarns being a stress concentrator, high enough to initiate break, d) the central yarn involved in contact is not yet broken and the stress distribution has lower values as compared to those characterizing the first layers.

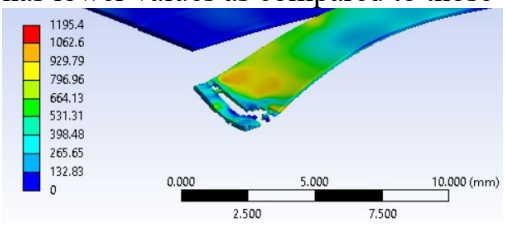

a) Layer 1

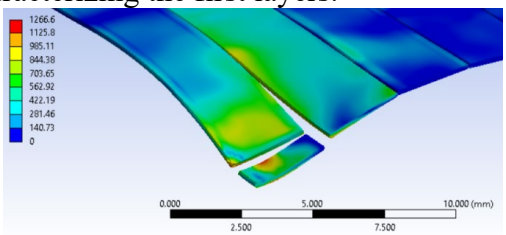

b) Layer 2

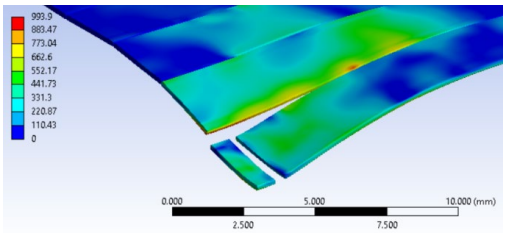

c) Layer 3

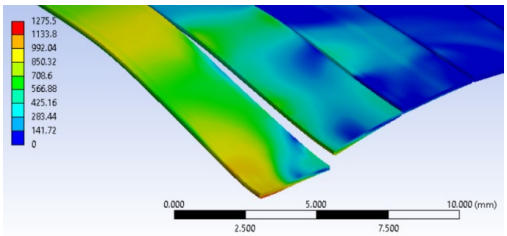

d) Layer 4

Fig. 10. Von Mises stress distribution (in MPa) and failure aspect at moment, $t=2.4\times10^{-5}$ s, $v_0=100$ m/s

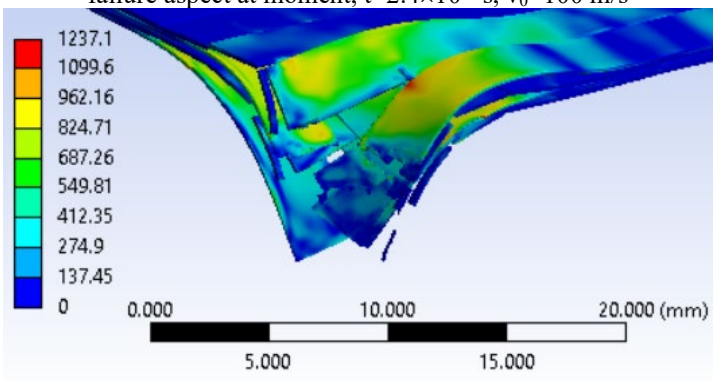

Fig. 11. Von Mises stress distribution (in MPa) and failure aspect at moment, $t=4\times10^{-5}$ s, $v_0=200$ m/s

At moment $t=4\times10^{-5}$ s (and impact velocity of $v_0=200$ m/s), the yarns next to the main yarns are broken, parallel to the width of the yarn (Fig. 11).

More details of yarns' failure are visible when a layer is kept visible, the others being invisible (Fig. 12). Also, this investigation of each layer points out the stress concentrators: a) the fragmentation has zig-zag edges of the yarn in the first layer and the contact between the broken yarn, bent outside the direct contact with the projectile, generates stress concentrator that will initiate the break on the next yarn, b) and on layer 2, yarn are not so bent, but in the quarter model, two yarns are broken and the yarn near those is already twisted and bent, producing stress concentrators in contact with its neighbor yarns, c) the central yarn is more bent, even if it is broken due to passing-by of the projectile, d) layer 4 has the main yarn more bent as there is no material behind it.

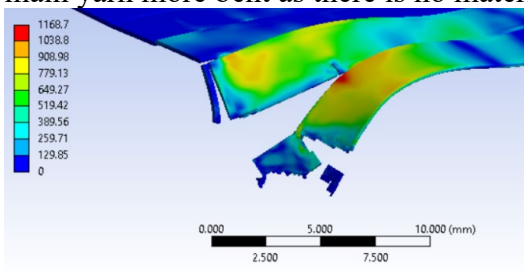

a) Layer 1

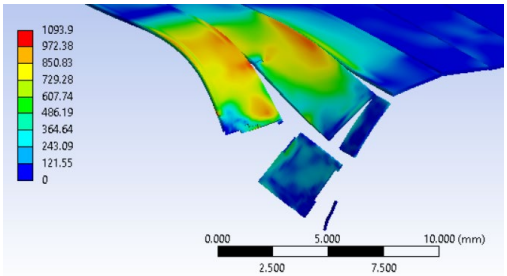

b) Layer 2

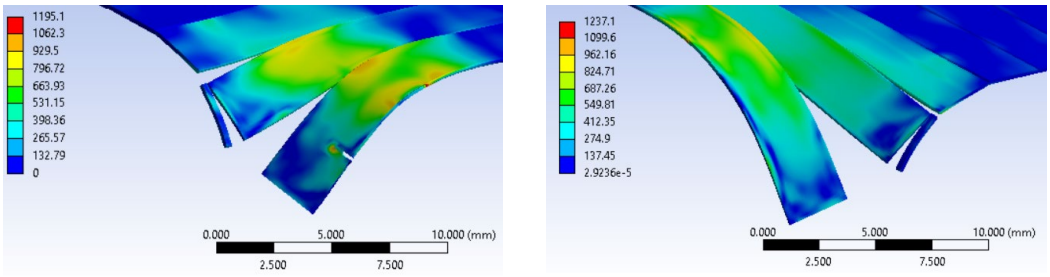

c) Layer 3 d) Layer 4

Fig. 12. Von Mises stress distribution (in MPa) and failure aspect of each layer, at moment $t=4\times10^{-5}$ s, $v_0=200$ m/s

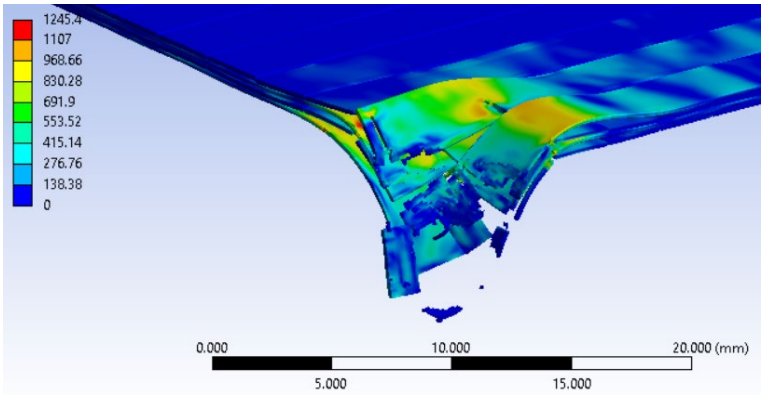

Fig. 13. Von Mises stress distribution and failure aspect at moment $t=2.4\times10^{-5}$ s, $v_0=300$ m/s

For the following simulations ($v_0=300$ m/s and $v_0=400$ m/s) the failure aspect is different (Fig. 13 and Fig. 15); less bending of the yarns and the break through yarns become almost circular. Details of each layer in Fig. 14 reveal: a) layer 1 has the central yarn broken in more fragments, it is strongly bent near the projectile and the yarn next to it is twisted, having a break due to the projectile and another partial break (yet) due to its forced position against the central yarn; b) and c) central yarns on layers 2 and 3 are fragmented and the yarns next them are twisted, d) the arching of the yarns is larger as there is no other layer to restrain their movement.

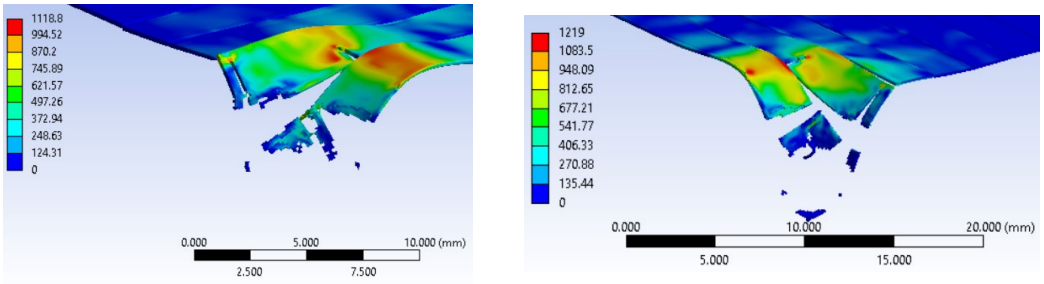

a) Layer 1 b) Layer 2

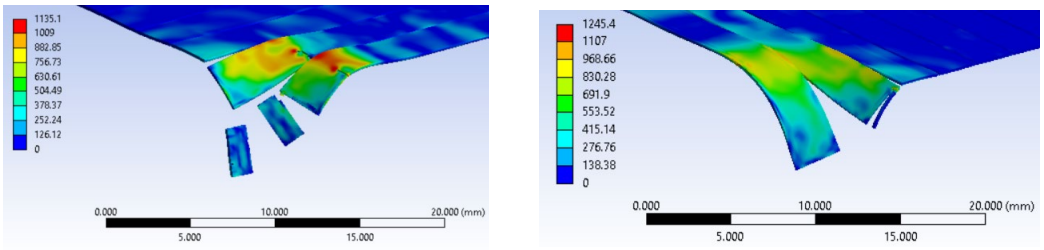

c) Layer 3 d) Layer 4

Fig. 14. Von Mises stress distribution (in MPa) and failure aspect at moment $t=2.4\times10^{-5}$ s, $v_0=300$ m/s

Under the highest impact velocity ($v_0=400$ m/s) the simulation was run, the aspect of broken yarns is more different as compared to that obtained with lower velocity ($v_0=100…200$ m/s), the boundary of the fragmented yarns is almost circular, but the bending is not so obvious (Fig. 15).

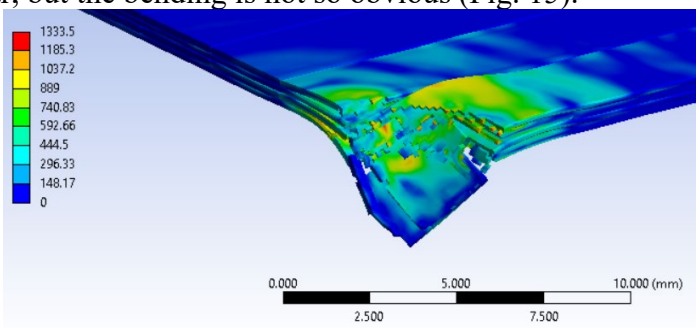

Fig. 15. Von Mises stress distribution (in MPa) and failure aspect at moment $t=8\times10^{-6}$ s, $v_0=400$ m/s

At the moment $t=8x10^{-6}$ s, layer 1 has the main yarn broken into several fragments, under the impact of the bullet (Fig. 16a). The yarn next to the main yarn is fragmented on the edge. On layer 1, the two central yarns involved in the contact are broken (in this quarter model but actually the system has three broken yarns) and they have high values of von Mises stress on very small areas. Yarns on layer 2 (Fig. 16b) are broken into several fragments, like layer 1. Main yarn on layer 3 (Fig. 16c) breaks into different size pieces, in a direction approximately parallel to the width of the yarn, the yarn next to the main yarn (that directly under the projectile) having stress concentrators. The main yarn in layer 4 (Fig. 16d) is partially broken and has a larger area with stress concentrators.

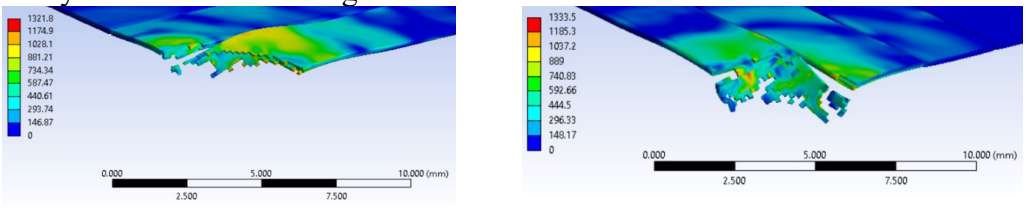

a) Layer 1 b) Layer 2

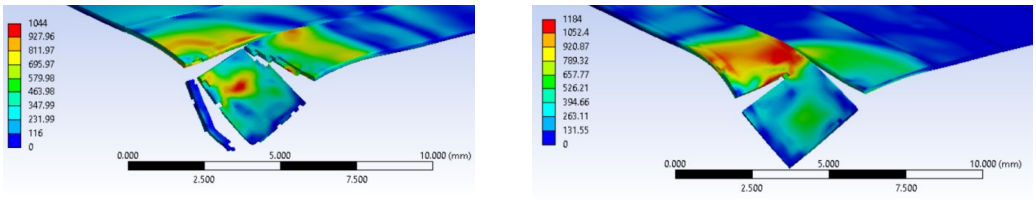

c) Layer 3 d) Layer 4

Fig. 16. Von Mises stress distribution (in MPa) and failure aspect at moment $t=8x10^{-6}$ s, $v_0=400$ m/s

5. Conclusions

If engineers designed a model including a geometry similar to actual application and with material constitutive models that are based on experimental data, the simulation results would help them to understand failure stages and mechanisms that are very difficult to be noticed during the tests due to the very short time of the impact process.

The paper presents an analysis of the failure stages and mechanisms for a package made of unidirectional glass fibers, in four layers, with alternative orientation (0º,90º,0º,90º), without matrix, but taking into account the friction among fibers and fibers and projectile. The constitutive models of the materials are taken from the recent literature, as isotropic bilinear ones. More complex constitutive models take into account the strain rate and the local temperature [11]-[13]. For instance, Naresh et al. [11] reported an increase of tensile limit for a 4-layer glass fiber/epoxy composite with 3% at a strain rate of 220 s^{-1} as compared to the value for a quasi-static test (0.001 s^{-1}). Young modulus is twice more that for quasi-static test, but for the higher strain rate, the strain at break decreased with 61%.

The simulation of the impact on a four-layer package pointed out the influence of impact velocity on maximum value of von Mises stress during the impact, on the acceleration of the bullet tip. The simulation allows for evaluating the residual velocity and comparing its values to those obtained in actual tests. Also, the aspect of broken yarns, even if for a compact yarn (not composed by numerous fibers), is similar to those obtained on SEM images for thicker packages using glass fiber fabrics.

Acknowledgement

This work has been supported by the European Social Fund through the Sectorial Operational Programme Human Capital 2014-2020, through the Financial Agreement with the title „Burse pentru educaţia antreprenorială în rândul doctoranzilor şi cercetătorilor postdoctorat (Be Antreprenor!)” "Scholarships for entrepreneurial education among doctoral students and postdoctoral researchers (Be Entrepreneur!)", Contract no. 51680/09.07.2019 - SMIS code: 124539

REFERENCES

[1] *A. Bhatnagar,* Standards and specifications for lightweight ballistic materials, in (Woodhead Publishing Limited, CRC Press, Boca Raton), pp. 127-167, 2006

[2] *** Opportunities in Protection Materials Science and Technology for Future Army Applications, National Academy of Sciences, ISBN 978-0-309-21285-4, 2011

[3] *P K Mallick, Fiber reinforced composites. Materials, Manufacturing and Design* (3rd ed), (CRC Press, Francis and Taylor Group), 2007

[4] *S. Sockalingam, S. C. Chowdhury, J. W. Gillespie Jr. and M. Keefe,* Recent advances in modeling and experiments of Kevlar ballistic fibrils, fibers, yarns and flexible woven textile fabrics – a review, Textile Research Journal, **vol. 87,** no. 8, pp. 984–1010, 2017

[5] *** Introduction of Glass Fiber. Types of Glass Fiber. Properties of Glass Fiber. Manufacturing Processes of Glass Fiber. Uses of Glass Fiber or Glass Yarn, http://textilelearner.blogspot.com/2011/08/glass-fiber-types-of-glass-fiber_3834.html

[6] *A. Endruweit, X. Zeng, M. Matveev and A. C. Long,* Effect of yarn cross-sectional shape on resin flow through inter-yarn gaps in textile reinforcements, Composites, Part A, 104, pp. 139-150, 2018.

[7] *S. Sockalingam, J. W Gillespie Jr. and M. Keefe*, Role of Inelastic Transverse Compressive Behavior and Multiaxial Loading on the Transverse Impact of Kevlar KM2 Single Fiber, in Fibers, **vol. 5,** no. 9, doi:10.3390/fib5010009, 2017

[8] *C. Pirvu, A. E. Musteata, G. G. Ojoc, S. Sandu and L. Deleanu*, A meso level FE model for the impact bullet - yarn, Revista de Materiale Plastice, **vol. 56**, no. 1, pp. 22-31, 2019

[9] *L. Chiper Titire*, Ballistic impact simulation on unidirectional glass fiber yarns and fabrics (in Romanian), disertation, "Dunarea de Jos" University, Galati, Romania, 2020

[10] *** Non-Crimp Glass Multiaxials, https://www.castrocompositesshop.com/en/80-non-crimp-glass-multiaxials

[11] *M. Karahan, A Kuş. and R. Eren*, An investigation into ballistic performance and energy absorption capabilities of woven aramid fabrics, International Journal of Impact Engineering, **vol. 35**, no. 6, pp. 499-510, 2008

[12] *G. Ojoc, L. Oancea, C. Pîrvu, S. Sandu and L. Deleanu*, Modeling of impact on multiple layers with unidirectional yarns, in Mechanical Testing and Diagnosis, **vol. 8,** no. 4, pp. 5-15. https://doi.org/https://doi.org/10.35219/mtd.2018.4.01, 2019

[13] *Catalin Pîrvu,* Contribuţii la studiul experimental și numeric al pachetelor de protecție balistică cu fibre aramidice, PhD thesis, Dunărea de Jos University, Galati, Romania, 2015

[14] *T.F. Ionescu, C. Pirvu, S. Badea, C. Georgescu and L. Deleanu*, The Influence of Friction Characteristics in Simulating the Impact Bullet - Stratified Materials, 15th International Conference on Tribology, Kragujevac, Serbia, 17 – 19 May 2017, 2017

[15] *K. Naresh, K. Shankar, B.S. Rao and R. Velmurugan*, Effect of high strain rate on glass/carbon/ hybrid fiber reinforced epoxy laminated composites, in Composites Part B, **100**, pp. 125-135, 2016

[16] *Y. Ou and D. Zhu*, Tensile behavior of glass fiber reinforced composite at different strain rates and temperatures, Construction and Building Materials, 96, pp. 648–656, 2015

[17] *N.K. Naik, P. Yernamma, N.M. Thoram, R. Gadipatri, V.R. Kavala*, High strain rate tensile behavior of woven fabric E-glass/epoxy composite, Polymer Testing, 29 pp. 14–22, 2010

[18] *A. Patnaik, P. Kumar and S. Biswas, M. Kumar,* Investigations on micro-mechanical and thermal characteristics of glass fiber reinforced epoxy based binary composite structure using finite element method, in Computational Materials Science, **vol. 62,** pp. 142–151, 2012

[19] *C. Ha-Minh, A. Imad, F. Boussu, T. Kanit and D. Crepin,* Numerical study on the effects of yarn mechanical transverse properties on the ballistic impact behaviour of textile fabric, in Journal of Strain Analysis, **vol. 47,** no. 7, pp. 524–534, doi: 10.1177/0309324712457901, 2012

[20] *E. Corona and B. Reedlun*, A Review of Macroscopic Ductile Failure Criteria, https://pdfs.semanticscholar.org/5404/27e7cd18762d80b311adc475825edf148a9b.pdf, 2013

[21] *G. G. Ojoc, L. Deleanu, C. Georgescu, D. Iorga, M. V. Popescu, C. Pîrv and S. Sandu,* Ballistic Panel Made of Glass Fiber Fabrics + Resin Matrix for Levels FB3 and FB5, the International Student Innovation and Scientific Research Exhibition, Cadet INOVA'20, Land Forces Academy, "Nicolae Balcescu", Sibiu, Romania, 2020